Edge Characterization of 3D Silicon Sensors after Bump-Bonding with the ATLAS Pixel Readout Chip

Ole Myren Røhne

***Abstract*—3D silicon sensors with electrodes penetrating the full substrate thickness, different electrode configurations and with active edges, where bump-bonded to the ATLAS pixel readout chip FE-I3 in 2006. Their characterization included electrical tests in laboratory, tests with beam and radioactive sources. Noise figures after bump bonding varied from 190 to 290 electrons, in agreement with the different electrode density of the three 3D configurations. This paper will reports beam results on the edge sensitivity, electrode response and efficiency at different angles of 3D sensors, fabricated at Stanford and bump-bonded to the ATLAS FE-I3 front end chip, before and after irradiation to 10^{15} high energy protons per cm^2.**

I. 3D Si Pixels for the LHC upgrade

A. Manufacturing technology and operating principles

Current state-of-the-art Deep Reactive Ion Etching (DRIE) allows for etched vertical structures with an aspect ratio $\mathrm{AR} = D/d$ in excess of 20. Full-3D active edge Silicon sensor technology combines DRIE technology with the materials and processing of conventional sensors manufacturing. The original idea and its implementation at Stanford, USA is described in [1][2]. The 3D sensors characterized here have matrices of fully penetrating vertical p- and n-electrode implants, as well an etched and implanted edge, which itself is an electrode, see figure 1. The active edge eliminates the guard rings associated with planar sensor designs, and the corresponding dead area at the edge is much reduced[3][4].This improves the overall material budget and the yield, and can be exploited in module designs with butted chip-size sensors tiles.

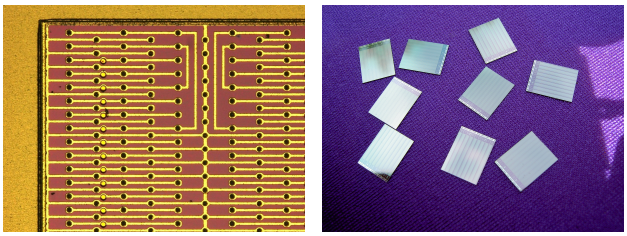

Fig. 1. Left: Detail showing column of edge pixels with the etched trench that defines the detector edge. Right: Etch-diced chip-size sensors, ready for tiling.

The lateral drift field (figure 2) between the vertical electrodes in 3D sensors geometrically decouples the total charge generated by a minimum ionizing particle from the inter electrode distance. After heavy irradiation the charge generated will suffer severe trapping by the radiation-induced defects in the silicon lattice. The reduced trapping distance will ultimately determine the signal efficiency, defined as the ratio between signals after and before irradiation. The above mentioned decoupling between substrate thicknesses and collection distance means that a 3D sensor can be optimized to retain excellent signal efficiency even after extreme radiation[5][6][7][8].

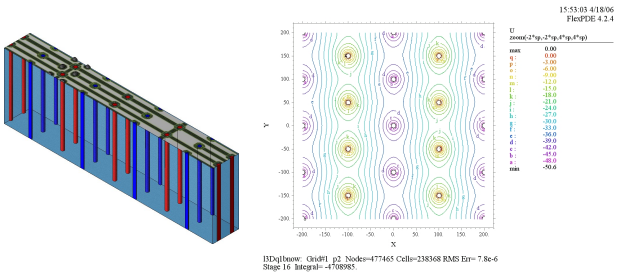

Fig. 2. Left: Pixel cells with n-type readout electrodes (blue) surrounded by p-type electrodes (red). Right: Field simulation showing equipotential lines.

B. ATLAS 3D Pixel R&D Collaboration:

Not preempting any lessons to be learned from operation during the initial low-luminosity phase of the LHC program, it seems clear that the most demanding requirements on pixel detectors at the SLHC will be to sustain the unprecedented radiation loads, and equally important, with a reduced radiation length, that is a smaller material budget. Looking toward the mid-life B-layer replacement, and a later SLHC upgrade, the ATLAS Pixel community is already evaluating a range of more-or-less aggressive technologies. In this context, full-3D active edge Silicon sensors seem particularly attractive because they provide the desired radiation hardness and a possibly reduced material budget while retaining compatibility with existing radiation hard electronics and module designs. A collaboration-approved R&D project has been formed[9]with an expressed purpose of

> "Development, Testing and Industrialization of Full-3D Active-Edge and Modified-3D Silicon Radiation Pixel Sensors with Extreme Radiation Hardness for the ATLAS experiment"

There are currently 13 participating institutions, working with 4 industrial partners, in addition to the original foundry MBC

University of Oslo
On behalf of the ATLAS 3D PixelCollaboration

at CIS-Stanford. The primary goal is the development, fabrication, characterization, and testing, with and without the front-end readout chip, of Full-3D active-edge and Mod-3D silicon pixel sensors of extreme radiation hardness and high speed for the Super-LHC ATLAS upgrade and, possibly, the ATLAS B-layer replacement. A secondary goal is to start design work for a reduced material B-layer detector module using these sensors.

C. Stanford 3D ATLAS Pixel compatible sensor

The 3D Pixel sensors under study in this paper were designed and manufactured by J. Hasi, (University of Manchester) and C. Kenney, (MBC at CIS-Stanford), with financial support from STFC, UK for the related FP420 project and DOE, USA for the ATLAS upgrade part of the project. Three different sensor layouts were included, characterized by having 2, 3 or 4 readout electrodes per $50\mu\mathrm{m} \times 400\mu\mathrm{m}$ ATLAS-compatible pixel. The 3E and 4E layouts relevant for this paper are detailed in figures 3 and 4. A prototype run on $210\mu\mathrm{m}$ p-type high-resistivity $12\mathrm{k}\Omega\mathrm{cm}$ silicon has been completed with 10 wafers; the yield evaluated on one wafer was close to 80%.

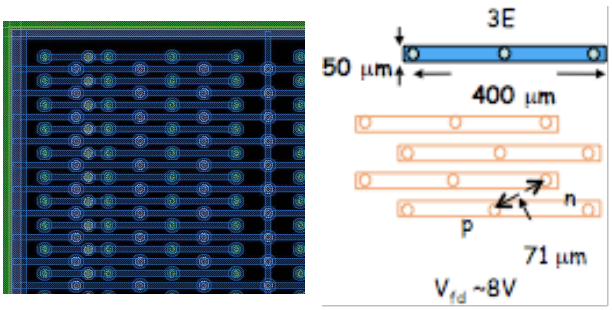

Fig. 3. Stanford 3D/3E sensor layout, 3 electrodes per pixel.

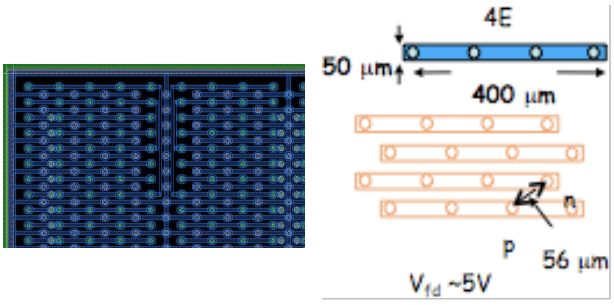

Fig. 4. Stanford 3D/4E sensor layout, 4 electrodes per pixel.

II. Sensor/electronics characterization

A. Test beam instrumentation

The CERN SPS North-area test beam provides minimum ionizing particles in the form of a $180\mathrm{GeV/c}$ $\pi^{\pm}$ beam, their high momentum minimizes multiple scattering in the experimental setup and makes them ideally suited for the characterization of high-precision tracking detectors. The data-taking took place over two weeks in June 2008, during which the SPS machine provided remarkably stable and consistent beam.

The trigger system uses the coincidence of several overlapping scintillators. For some of the runs a downstream veto-counter with a $15\mathrm{mm}$ aperture was added to suppress showering events. For the purpose of studying sensor/electronics timewalk, the phase of each trigger with respect to a free-running $40\mathrm{MHz}$ "LHC"-clock was recorded with a sub-ns resolution time digitization counter (TDC).

The beam-telescope consisted of 3 planes of $50\mu\mathrm{m}$ pitch double-sided Silicon strip detectors, provided by Bonn University. Tracks were reconstructed from events having exactly one hit in each of the telescope planes. An initial optical alignment was provided by CERN's North-area survey group, final alignment was done using registered tracks.

For a preliminary evaluation of the tracking resolution the superimposed image of single-pixel hits in the device under test (DUT) have been fitted with a box response convoluted with a Gaussian resolution, yielding an upper limit on the extrapolated track resolution of about $11\mu\mathrm{m}$. An earlier characterization by M. Mathes and coworkers [10], using essentially the same instrumentation, reports a much better resolution of $5-6\mu\mathrm{m}$. This discrepancy is partly due to the previous setup having one more tracking plane but probably also reflects a residual misalignment in the present track reconstruction.

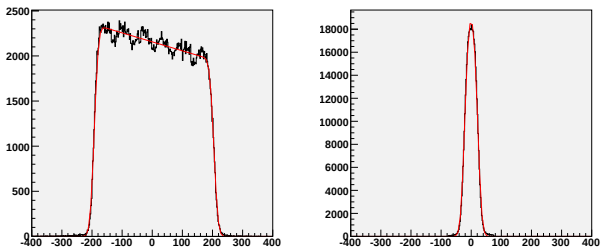

Fig. 5. Superimposed images of single-pixel hits, projected onto the pixel column (left) and row (right) axes. The fit functions are the expected box response convoluted with a Gaussian resolution, the fit yields $\sigma = 11\mu\mathrm{m}$. The slope at the top of the column response is due to the non-flat beam profile, the peaks and troughs are due to the inefficiencies at the electrode columns.

B. Interior pixel response

A possible hit inefficiency due to tracks passing through the potentially dead column area is a concern for 3E pixel sensors. A previous study [10] has found the average inefficiency for normal incidence to be compatible with expectations considering the fraction of the sensor area covered by electrodes, and shown that the efficiency approaches 100% for tracks at 15° incidence.

When the signal of a hit is shared among two or more pixels, only a fraction of the total signal is available for each

comparator to go above threshold. In order to retain maximum efficiency as the available signal decrease with the onset of radiation damage, it is desirable to minimize charge sharing. This is in contrast to sensor designs that are optimized for resolution, often intentionally enhancing charge sharing. The cage-like bias electrode configuration of a 3D pixel sensor naturally has very little charge sharing for particles of normal incidence - perhaps except for narrow regions along the long pixel edge and away from the electrodes.

The hit efficiency is evaluated considering the number of tracks with registered hits in the device under test and the total number of tracks passing through a region of the sensor. Similarly, the charge sharing probability is defined as the number of tracks with hits in more than one pixel cell divided by the total number of tracks with hits passing through a region of the sensor. The results for 3D/3E and 3D/4E sensors, both with a bias of $40\mathrm{V}$, are shown in figures 11 and 7, respectively. Key observations are efficiencies in excess of 90%, and the confirmation that tracks passing close to a readout column yield a distinct secondary peak in the charge distribution.

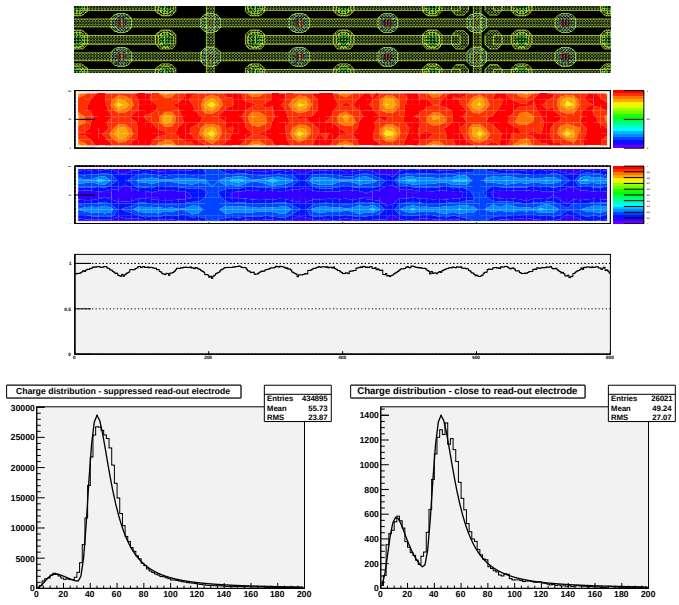

Fig. 6. Stanford 3D 3E interior pixel response, normal incidence, bias $40\mathrm{V}$. From top to bottom: Mask detail, $800\mu\mathrm{m}\times100\mu\mathrm{m}$ centered on a pixel cell. Hit efficiency map across corresponding area. Charge sharing probability across corresponding area. Hit efficiency projection onto the horizontal axis. Pulse height distribution, bulk region (left) electrode region (right). The average hit efficiency is 92% (prelim). The average charge sharing probability is 14% (prelim). The peak of the secondary Landau in the electrode region is at 27.2% of the charge in the main peak.

C. Active edge response

Considering that 3D technology requires that the sensor edge is doped and connected to the bias grid, the sensor is expected to be fully efficient all the way to the edge. In view of the possibility of building detector modules from butted chip-size sensor tiles it is desirable to make the edge pixels slightly wider than interior pixels in order that the sensor can overlay the bump-bonded readout chip. In order to maintain inter-electrode spacing the edge pixels have one extra readout electrode compared to interior pixels. The edge response for the 3E and 4E layouts has been extracted by fitting the hit efficiency with a step function convoluted with a Gaussian resolution as shown in figures 8 and 9, the results are summarized in table I The observed edge positions are compatible with as-built sensor geometry. Due to experimental tracking resolution the shape of the edge is indistinguishable from a completely sharp transition region.

	3E	4E	
Nominal width	533.0	517.0	μm
Fitted width	531.9	517.5	μm
Fitted resolution	12.0	10.5	μm

TABLE I
STANFORD 3D 3E AND 4E ACTIVE EDGE RESPONSE.

D. Sensor capacitance and in-time efficiency

When operating in a clocked and triggered environment like the LHC, it is important that any pixel hit gets assigned to the correct bunch collision; otherwise if the time walk exceeds the bunch collision period the result is a loss of efficiency.

Measurements (C. DaVia, IEEE NSS 2007) indicate that the capacitance plateau is reached only well above the theoretical full depletion voltage. The eventual capacitance and resulting timewalk/overdrive is higher than for planar devices. Some mitigation of the efficiency loss expected as the 3D sensors also exhibit less charge sharing compared to planar sensors.

For the current ATLAS Pixel detector the time walk requirement has been specified in terms of the related threshold *overdrive*: The amount of excess charge above threshold required for the comparator to fire within $20\mathrm{ns}$ of a high-amplitude ($100\mathrm{fC}$) reference signal. The overdrive is normally measured by injecting known charges and scanning the signal arrival time; this procedure requires some adaptions to be applied in a test beam environment: The known injected charge is replaced by the measured Time-over-Threshold, and the non-synchronous beam provides a sample of different arrival times.

	Planar, 150V	4E, 40V	4E, 15V	
Noise (full bias)	180	290	340	e^-
Overdrive (lab)	1244	3340	-	e^-
Overdrive (beam)	-	3920	5040	e^-

TABLE II
STANDARD ATLAS PIXEL AND STANFORD 3D 4E SENSORS NOISE AND OVERDRIVE, MEASURED USING INJECTED CHARGE AND WITH CHARGED PARTICLES.

III. Irradiation test

In a first attempt at demonstrating 3D sensor radiation hardness with realistic LHC-type electronics, a Stanford 3D 3E device bump bonded to an ATLAS Pixel FE-I3 front-end asic was irradiated under with $24\mathrm{GeV}$ protons in the CERN PS Irradiation facility. The accumulated fluence was $9.8{\cdot}10^{14} mathrm cm^{-2}$, which is approximately equivalent to $5{\cdot}10^{14}\mathrm{cm}^{-2}$ $1\mathrm{MeV}$ neutrons. The irradiation was performed under $40\mathrm{V}$ bias, and the sensor was partially annealed prior to testing. Due to various mishaps during the subsequent handling the specimen turned out to develop a low-voltage break-down which limited the bias voltage below $5\mathrm{V}$. Operating at with cooling limited to $0\mathrm{degC}$ the sensor were still capable of registering register minimum ionizing particles, with an efficiency of 20.9%.

IV. Conclusion and outlook

Stanford 3D detectors bump-bonded to the ATLAS FE-I3 readout chip have been successfully tested in a $180\mathrm{GeV/c}$ $\pi^{\pm}$. beam in June 2008. The edge response of 3E and 4E electrode configurations has been measured to be $\sigma = 10 - 12\mu\mathrm{m}$, probably dominated by contributions from tracking resolution and residual misalignment. A 3E assembly was irradiated to $9.8{\cdot}10^{14}\mathrm{cm}^{-2}$ $24\mathrm{GeV}$ protons. With less than $5\mathrm{V}$ bias at a temperature of $0\mathrm{degC}$ the region in the center of the pixel cell still retains some efficiency to charged particles.

V. Acknowledgment

These measurements would not have been possible without the dedicated work of the following groups and individuals:

The CERN SPS and North Area teams.

Maurice Glaser at the CERN PS Irradiation facility.

Ian McGill at the CERN PH Deptartment Silicon Facility.

The ATLAS Test beam coordinator Beniamino Di Girolamo.

For sensor bump-bonding and mounting, Bonn University with IZM Berlin.

The test beam set-up and operation team: E. Bolle, B. Buttler, C. Da Via, O. Dorholt, S. Fazio, H. Gjersdal, J. Hasi, A. La Rosa, C. Kenney, D. Miller, C. Young, V. Linhart, H. Pernegger, T. Slavicec, K. Sjobak, M. Tomasek, S. Watts

References

[1] S. I. Parker, C. J. Kenney, and J. Segal, "3-D: A New architecture for solid state radiation detectors," *Nucl. Instrum. Meth.*, vol. A395, pp. 328–343, 1997.

[2] C. Kenney, S. Parke, J. Segal, and C. Storment, "Silicon detectors with 3-D electrode arrays: Fabrication and initial test results," *IEEE Trans. Nucl. Sci.*, vol. 46, pp. 1224–1236, 1999.

[3] C. Kenney, S. Parker, and E. Walckiers, "Results from 3-d silicon sensors with wall electrodes: near-cell-edge sensitivity measurements as a preview of active-edge sensors," *Nuclear Science, IEEE Transactions on*, vol. 48, no. 6, pp. 2405–2410, Dec 2001.

[4] C. Kenney, J. Segal, E. Westbrook, S. Parker, J. Hasi, C. Da Via, S. Watts, and J. Morse, "Active-edge planar radiation sensors," *"Nucl. Instrum. Meth."*, vol. A565, pp. 272–277, 2006.

[5] S. Parker and C. Kenney, "Performance of 3-d architecture silicon sensors after intense proton irradiation," *Nuclear Science, IEEE Transactions on*, vol. 48, no. 5, pp. 1629–1638, Oct 2001.

[6] S. Parker, G. Anelli, C. Da Vi, J. Hasi, P. Jarron, C. Kenney, A. Kok, E. Perozziello, and S. J. Watts, "Advances in silicon detectors for particle tracking in extreme radiation environments," *Nucl. Instrum. Methods Phys. Res., A*, vol. 509, pp. 86–91, 2003.

[7] T. Lari, "Radiation hardness studies of silicon pixel detectors," *Nucl. Instrum. Methods Phys. Res., A*, vol. 560, no. 1, pp. 93–97, 2005.

[8] C. Da Via *et al.*, "Radiation hardness properties of full-3D active edge silicon sensors," *Nucl. Instrum. Meth.*, vol. A587, pp. 243–249, 2008.

[9] C. Da Via, S. Parker, and G. Darbo, "Development, testing and industrialization of full-3d active-edge and modified-3d silicon radiation pixel sensors with extreme radiation hardness results, plans." *ATLAS Upgrade*, 2007. [Online]. Available: http://atlas-highlumi-3dsensor.web.cern.ch/atlas-highlumi-3dsensor/WorkDocuments/ATLAS_3D-Sensor_proposal.pdf

[10] M. Mathes *et al.*, "Test beam Characterizations of 3D Silicon Pixel detectors," *arXiv*, 2008.

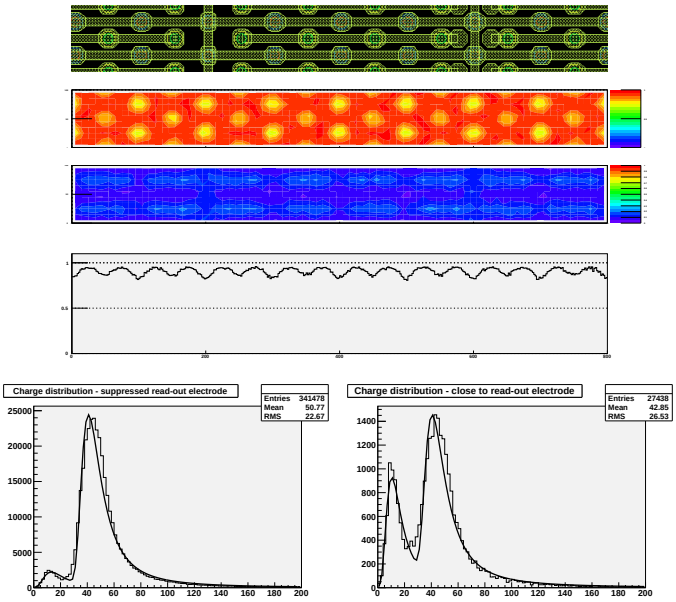

Fig. 7. Stanford 3D 4E interior pixel response, normal incidence, bias 40V. From top to bottom: Mask detail, $800\mu\text{m}\times100\mu\text{m}$ centered on a pixel cell. Hit efficiency map across corresponding area. Charge sharing probability across corresponding area. Hit efficiency projection onto the horizontal axis. Pulse height distribution, bulk region (left) electrode region (right). The average hit efficiency is 90% (prelim). The average charge sharing probability is 11% (prelim). The peak of the secondary Landau in the electrode region is at 26.7% of the charge in the main peak.

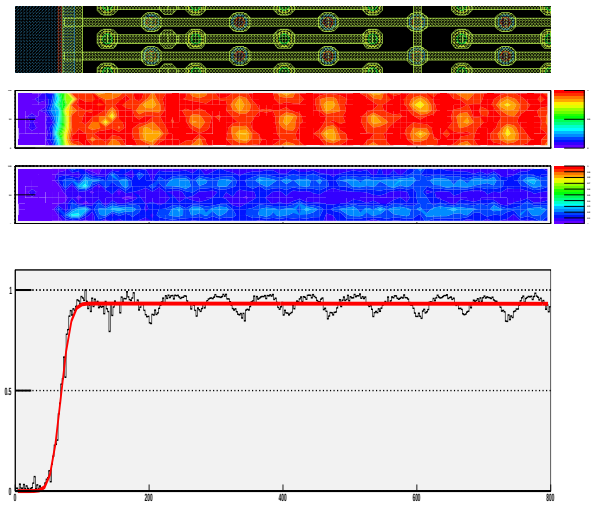

Fig. 8. Stanford 3D 3E active edge response, normal incidence, bias 40V. From top to bottom: Mask detail, $800\mu\text{m}\times100\mu\text{m}$ centered on an edge pixel. Hit efficiency map across corresponding area. Charge sharing probability across corresponding area. Hit efficiency projection onto the horizontal axis. The fitted function is a step response convoluted with a Gaussian resolution. The extracted edge position corresponds to a pixel width of $\mu = 531.9\mu\text{m}$, and the slope of the edge has a resolution $\sigma = 12.0\mu\text{m}$.

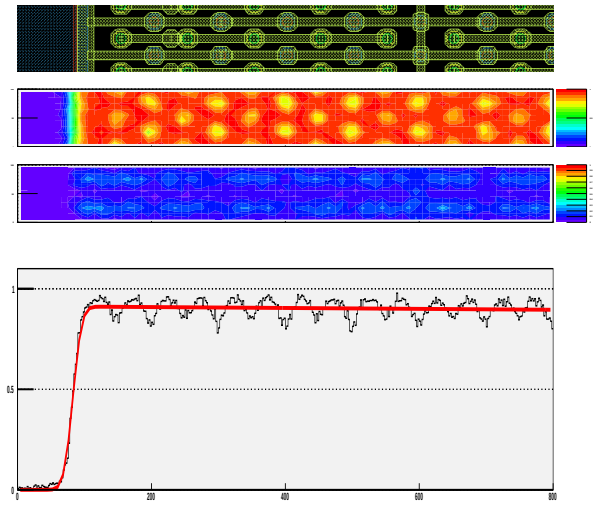

Fig. 9. Stanford 3D 4E active edge response, normal incidence, bias 40V. From top to bottom: Mask detail, $800\mu\text{m}\times100\mu\text{m}$ centered on an edge pixel. Hit efficiency map across corresponding area. Charge sharing probability across corresponding area. Hit efficiency projection onto the horizontal axis. The fitted function is a step response convoluted with a Gaussian resolution. The extracted edge position corresponds to a pixel width of $\mu = 517.5\mu\text{m}$, and the slope of the edge has a resolution $\sigma = 10.5\mu\text{m}$.

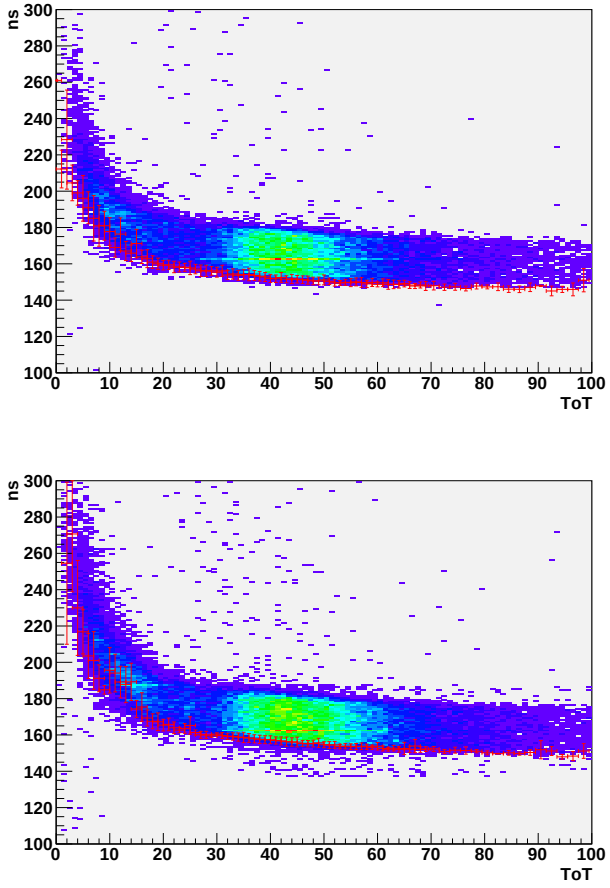

Fig. 10. Stanford 3D 4E hit arrival versus signal charge (ToT) at different bias voltages: 40V (top) and 15V (bottom). For each slice of signal charge the leading edge is fitted (red crosses). The overdrive is defined as the charge required for the leading edge to appear within 20ns of the asymptotic (high charge) value.

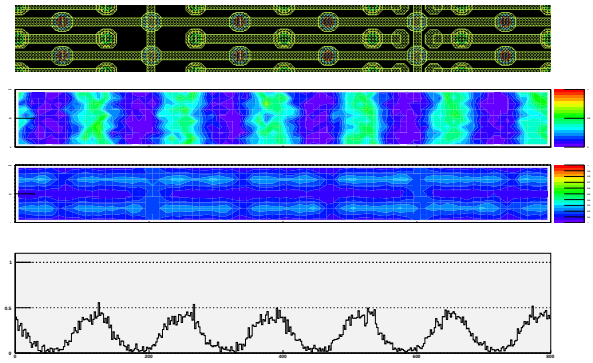

Fig. 11. Stanford 3D 3E irradiated detector response, bias below 5V. From top to bottom: Mask detail, $800\mu\mathrm{m}\times100\mu\mathrm{m}$ centered on a pixel cell. Hit efficiency map across corresponding area. Hit efficiency projection onto the horizontal axis. The average hit efficiency is 20.9% (prelim).